

Natural segmentation of the locomotor behavior of drug-induced rats in a photobeam cage

Neri Kafkafi^{a,c,*}, Cheryl Mayo^c, Dan Draï^b, Ilan Golani^b, Greg Elmer^c

^a National Institute on Drug Abuse, Baltimore, MD, USA

^b Tel-Aviv University, Tel-Aviv, Israel

^c Maryland Psychiatric Research Center, University of Maryland, Baltimore, MD, USA

Received 19 January 2001; received in revised form 22 May 2001; accepted 23 May 2001

Abstract

Recently, Draï et al. (*J Neurosci Methods* 96 (2000) 119) have introduced an algorithm that segments rodent locomotor behavior into natural units of 'staying in place' (lingering) behavior versus going between places (progression segments). This categorization, based on the maximum speed attained within the segment, was shown to be intrinsic to the data, using the statistical method of Gaussian Mixture Model. These results were obtained in normal rats and mice using very large (650 or 320 cm) circular arenas and a video tracking system. In the present study, we reproduce these results with amphetamine, phencyclidine and saline injected rats, using data measured by a standard photobeam tracking system in square 45 cm cages. An intrinsic distinction between two or three 'gears' could be shown in all animals. The spatial distribution of these gears indicates that, as in the large arena behavior, they correspond to the difference between 'staying in place' behavior and 'going between places'. The robustness of this segmentation over arena size, different measurement system and dose of two psychostimulant drugs indicates that this is an intrinsic, natural segmentation of rodent locomotor behavior. Analysis of photobeam data that is based on this segmentation has thus a potential use in psychopharmacology research. © 2001 Elsevier Science B.V. All rights reserved.

Keywords: Open field; SEE; Lowess; Exploratory behavior; Stops; Amphetamine; Phencyclidine

1. Introduction

The measurement of locomotor activity in rodents is one of the most widespread behavioral tests used in psychopharmacology and neurobiology. The most common method for measuring it employs infrared photobeams in a small test cage, and several such systems are available commercially. The standard analysis of photobeam results, however, usually employs general cumulative measures of activity (e.g. the number of beam breaks or, in the more advanced systems, the total distance traveled), cumulative time spent in the center of the chamber, etc. Such measures reflect the underlying notion that locomotor activity is rather stochastic in nature. Frequently, the ability of these measures to discriminate between, e.g. different genotypes, drugs,

doses, and experimental treatments is rather limited.

A more advanced approach developed by Paulus and Geyer (1991), Paulus et al. (1990) assumes that locomotor behavior in the photobeam cage is in fact structured and patterned, and the appropriate measures should reflect this structure. The measures used by this method, such as the entropy and the fractal dimension of the path, are based on general considerations of dynamical systems theory. This method was proved to have more discriminative power than the usual activity analysis. Due to the generality of this approach, however, it is sometimes difficult to interpret its results in specific cognitive, psychological or ethological terms.

The detailed structure of rat locomotor behavior, especially under various pharmacological, neurological and genetic manipulations, was studied in the open field (e.g. Gingras and Cools, 1997; Cools et al., 1997; Szechtman et al., 1998; Whishaw et al., 1994), and in various other setups that measure spatial behavior (e.g. Morris, 1984; Whishaw et al., 1993). Since studies

* Corresponding author Tel.: +1-410-550-1601; fax: +1-410-550-1612.

E-mail address: nkafkafi@intra.nida.nih.gov (N. Kafkafi).

utilizing the photobeam cage, however, do not usually analyze their data in spatial terms, they can neither contribute nor draw from this body of knowledge. This is not due to any technical problem, since at least some of the currently available photobeam systems can export raw coordinate files, but because of the inherent complexity of this analysis. Software for spatial analysis of photobeam data may thus remedy this problem.

In recent years, an ethological study of the structure of the path traveled during exploratory behavior of rats in large (several meters size) arenas revealed that it consists of distinctive patterns. The most basic of these patterns are ‘stops’ and ‘progression segments’, serving as the basic units or ‘primitives’ of the structure. More complex patterns such as ‘principal places’, ‘home base’ and ‘excursions’ (Eilam and Golani, 1989; Golani et al., 1993; Tchernichovski and Golani, 1995; Tchernichovski et al., 1989) are defined by the spatial and sequential organization of these primitives. Recently, specialized software called Software for the Exploration of Exploration (SEE) was developed by Draai and Golani (2001) for visualization and quantification of these patterns out of the automatically measured path. SEE analysis may prove a useful complementary approach because it quantifies specific movement patterns that are usually easier to visualize and interpret in ethological and psychological terms.

Although it is apparent even to the untrained observer that the progression of a rat into a novel environment typically consists of bouts and stops, the algorithmic definition and automatic recognition of these primitives in the time series of the animal’s coordinates has not been straightforward. This is because a stop does not necessarily imply zero speed. As a matter of fact, during a so-called stop a rat may perform many ‘local’ movements, such as scanning movements, rearing, backward and sideway steps, etc. In order to show that the categorization of the behavior into ‘stops’ and ‘progression segments’ is the result of a natural distinction, and not an arbitrary partitioning imposed over a continuum, it was necessary to demonstrate that the

distribution of the speed, or some similar measure, is typically multi-modal. Such multi-modality has recently been shown by Draai et al. (2000) for both rats and mice in a large arena.

The procedure suggested by Draai et al. (2000) for the segmentation of spatial behavior into stops and movement segments consists of two steps. In the first step, segments of ‘non-arrest’ are defined as those in which the speed is higher than the measurement noise of the tracking system (Fig. 1). Each of these segments is specified by the maximum speed attained within it. In the second step, the distribution of these maxima is analyzed. An unexpected result was that this distribution is typically not bi-, but tri-modal. The significance of three different components in the distribution was shown by using the statistical method of Gaussian Mixture Model. This method models the distribution as a sum of several normal distributions (Fig. 2). Sequences that include only alternation between segments belonging to the slower component (‘1st gear’, G1) and arrest segments (that were filtered out at the first stage) were termed ‘lingering episodes’. Lingering episodes were shown to be spatially localized, covering distances of rarely more than one rat length. In other words, although there is no a-priori reason preventing a rat from covering a long distance in the lingering mode, it in fact hardly ever does so in the context of exploratory behavior in a novel environment. Lingering episodes coincide very well with the subjective notion of stops, as would be recognized in the videotape by an experienced observer. Segments of the mid-speed component (‘2nd gear’, G2) cover longer distances, typically around one rat length, while segments of the high-speed component (‘3rd gear’, G3) cover distances ranging from several rat lengths up to several meters (limited only by arena size). This segmentation of the animal’s path thus supplied operative definitions of ‘within place behavior’ versus ‘going between places’. The spatial aggregation of several non-consecutive lingering episodes can now be used to operatively define the cognitive notion of ‘a place’. The more complex pat-

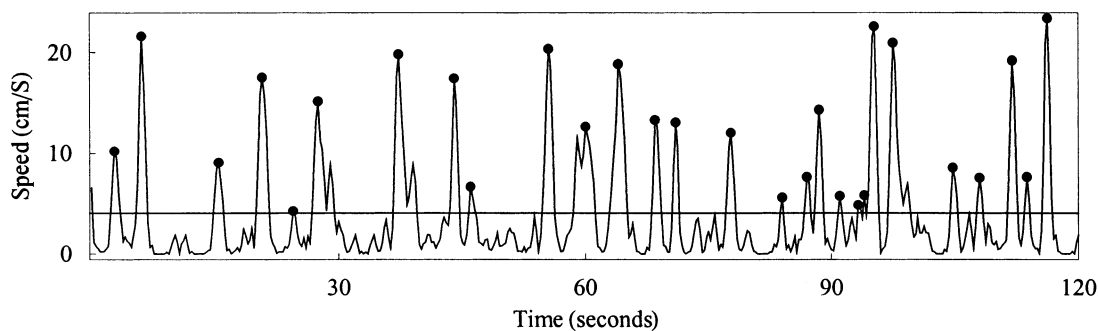


Fig. 1. A time-series of movement speed during 2 min out of a 5.0 mg/kg amphetamine-injected rat photobeam session. The horizontal line denotes the 4 cm/s threshold of estimated measurement error. Any speed value below this threshold is considered in this study as arrest. ‘Non-arrest’ segments are each specified by the maximum speed attained within this segment (black dots).

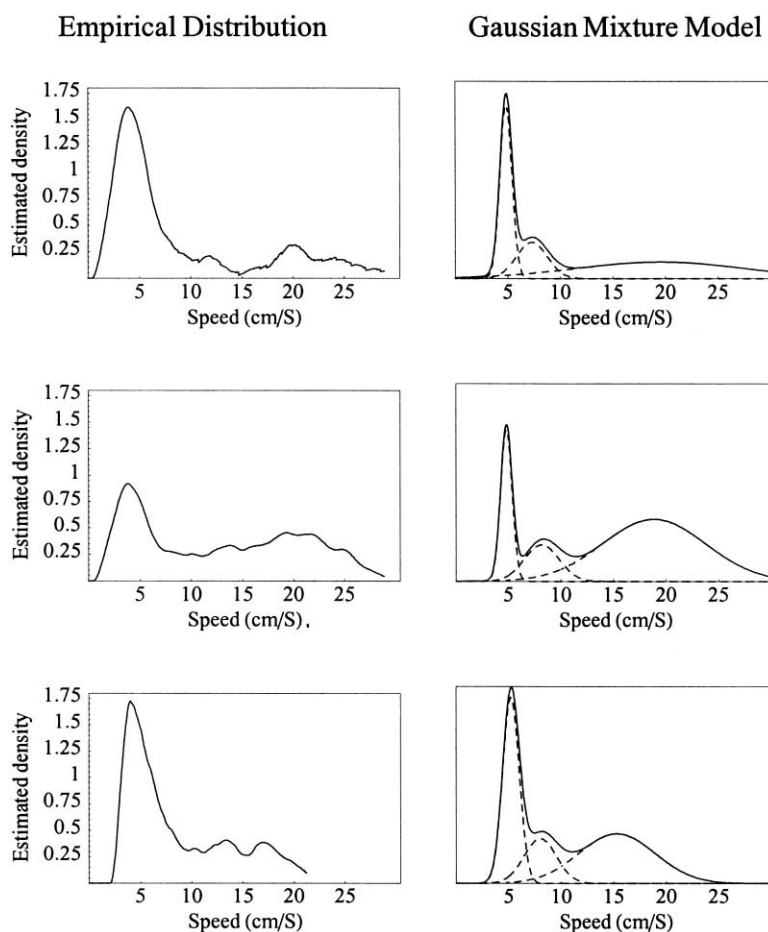


Fig. 2. Left, the empirical distribution of segment maximum speed, using the density estimation curve, in a 60 min session of one saline-injected rat (top), one 5.0 mg/kg amphetamine-injected rat (middle) and one 10.0 mg/kg PCP-injected rat (bottom). Right, the maximum likelihood Gaussian Mixture Models of the corresponding distributions on the left. Dashed lines show the individual Gaussian components. The solid line shows the sum (i.e. the mixture) of the Gaussians. In both cases shown here, the addition of the third component to the model increased the likelihood significantly (at 0.01 level), while additional components did not.

terns of exploratory behavior that were earlier mentioned can likewise be defined algorithmically (and measured automatically) as compositions of stops (i.e. lingering episodes) and progression segments (i.e. G2 and G3). Such algorithmic definition is the basis for the framework of SEE (Drai and Golani, 2001).

It is, therefore, clear that SEE analysis has a high potential for augmenting the methods of locomotor behavior analysis currently in use in psychopharmacology, by automatically recognizing and quantifying patterns that were shown to have intrinsic meaning for the animal. Such patterns are relatively easy to interpret in cognitive and psychological terms.

SEE analysis, however, crucially depends on the segmentation of the path into its primitives of stops and movement segments, i.e. on the existence at least two components in the distribution of speed maxima. It is essential, therefore, to determine how general these components are, and how independent they are of arena size, experimental protocol and tracking system properties. Here we report the application of speed

segmentation to data of drug-injected rats, measured by a standard photobeam chamber 43 cm wide.

About 35 days old Sprague–Dawley rats were injected with four doses of d-amphetamine (AMPH) and five doses of phencyclidine (PCP), and their locomotor behavior was measured for 1 h in standard 'Tru-Scan' photobeam chambers. The coordinates of the path were exported and analyzed by a SEE program, using the same segmentation procedure previously described, in order to determine if similar components in the distribution of speed maxima exists, and if their spatial distribution is similar to the one found in data from large arenas.

Photobeam systems are widely available, and at least some of the new systems are able to export the coordinates of the path as ASCII files for analysis. A demonstration of segmentation in such data will enable the application of SEE to its analysis. Such an application has a high potential for use in psychopharmacology and behavior genetics research.

2. Methods

2.1. Animals

Subjects used in this experiment were male Sprague–Dawley rats (Charles River Laboratories) weighing 100–125 g. The animals were housed in trios in clear plastic cages with wire grid lids. Access to food and water was unrestricted. The animals were kept in the animal facility maintained on a 12-h light: 12-h dark cycle (lights on at 19:00 h). The animals used in this study were maintained in facilities fully accredited by the American Association for the Accreditation of Laboratory Animal Care (AAALAC) and the studies were conducted in accordance with the Guide for Care and Use of Laboratory Animals provided by the NIH.

2.2. Locomotor activity measurement

All subjects received one injection of either drug or saline on the treatment day. The animals were brought down from the animal facility and placed in a holding room for 60 min. Each subject was weighed and marked. After 60 min each animal was placed immediately in the activity monitor for a 30 min baseline without drug. After a 30 min period, the session automatically paused. During this interval, each subject received an injection of saline, PCP or AMPH and was placed back into the locomotor activity monitor for 70 min. Each animal was used only once for each drug and dose. All injections were given intraperitoneal (i.p.) in an injection volume of 1 ml/kg body weight. PCP and AMPH were dissolved in 0.9% sodium chloride. Doses and number of animals in the PCP group were—saline, five animals; 1 mg/kg, six animals; 3 mg/kg, seven animals; 5 mg/kg, eight animals; 10 mg/kg, ten animals. Doses and number of animals in the AMPH group were—saline, seven animals; 1.5 mg/kg, 11 animals; 3 mg/kg, 12 animals; 5 mg/kg, 12 animals. Animals were assigned to each dose condition in a manner that resulted in each cage having several dose conditions. Station assignments were distributed such that each locomotor activity station ran an equal number of drug and dose conditions. Within each session all doses of the drug were represented.

Locomotor activity was monitored in Coulbourn Instruments' Tru Scan Activity Monitors. Animals were placed in a square (43 × 43cm) Plexiglas retainer. Activity in the monitor was recorded by photobeam interruptions. A ring of sensors, spaced 2.54 cm from each other, measured the X–Y location of the animal four times per second. The activity monitor computed the location of the animal in each of the X and Y dimensions as the middle point between the extreme beam interruptions in this dimension.

2.3. Analysis methods

Data were analyzed by the same algorithms developed for a large arena, using a video tracking system (Drai et al., 2000). Raw data files of the coordinates were exported from the photobeam cage, using 'TruScan' software. These files are ASCII files, which can be imported into Mathematica, the programming environment in which SEE resides. After computation of movement speed, segments having higher speeds than the system's noise level were filtered (Fig. 1), and the distribution of their maximal speeds were analyzed using the Gaussian Mixture Model (Fig. 2).

There were only two differences between the process of analysis used in this study and the one used in Drai et al. (2000). First, speed was estimated by the Lowess method, rather than the 'local movement' method, for reasons that will be explained in the next section. Second, the Gaussian Mixture analysis was performed on the distribution of speed maxima themselves, rather than on the distribution of the log-transformed speed maxima, as in Drai et al. (2000). The reason for this is that in the large arena rats can develop much higher speeds, so that the range of speeds extends over almost two orders of magnitude. The range of G2 and especially G3 speeds extended over several times more than the range of G1 speeds, so that a log-transformation was necessary to elucidate the multi-modality of the distribution. In contrast, the range of speeds in the small photobeam chamber was less than one order of magnitude, thus making the log-transformation inappropriate. In fact, in most of the rats in this study, we got similar results while using log-transformation. Only in some of the less active rats (and thus having a smaller range of speeds) the log-transformation masked the multi-modality of the distribution. We, therefore, omitted the log transformation, as to enable comparison among all animals.

The Lowess method for the computation of speed will be explained here in more detail since this is the first account of its use in the segmentation of locomotor behavior. For a detailed description of the other methods see Drai et al. (2000).

2.3.1. Lowess smoothing and velocity estimation

Drai et al. (2000) estimated the speed by computing the standard deviation (S.D.) of the distances of the data points to their mean within a sliding time window 0.4 s wide, constructed around each data point in turn (S.D. method). Here we employed a more robust and exact way for both smoothing measurement noise and estimation of the speed, namely Locally Weighted Estimation and Smoothing Scatter plots ('Lowess', see Cleveland, 1977). The use of Lowess is especially crucial in this study since our segmentation is based on the analysis of speed, which is even more subject to mea-

surement noise than the coordinates of the path. This is because any method of estimating the speed in a given time point t_i depends on measuring the coordinates in at least two time points (e.g. the difference between the coordinates at times t_i and t_{i-1}), thus adding up the noise components of these measurements. In addition, Lowess is a robust method that automatically disregards ‘outliers’, i.e. data points that fall very far from most nearby points, and are clearly a result of some artifact in the measurement or analysis system. With non-robust smoothing methods, such as moving averages or the S.D. method, such data points will greatly affect the location and velocity estimation of neighbor time points.

Lowess uses a sliding time window, constructed in turn around each data point. In the first iteration, data points within each time window are fitted with a polynomial using least-square optimization. In order to prevent artificial discontinuities generated by the border of the time window, the least-square optimization is weighted by a smooth weight function that has a maximal value at the center of the time window (i.e. at the point around which it was constructed) and descends to zero at its borders. The value of the optimal polynomial at the center of each window is used as a first estimation of the data point around which the window is centered. In addition, we used the slope of the polynomial at the center as a first estimation for the velocity at the respective data point. In the second iteration, step one is repeated, but this time data points are also weighted by the absolute difference between them and the first estimation. Data points that are far enough (more than six medians of the absolute estimation error) from the first estimation are considered ‘outliers’ and get a zero weight, i.e. they will be completely disregarded from computing the new estimation within each time window. Values and slopes of the new polynomials constitute the second estimation for the location and velocity in the respective data points. It is possible to repeat this procedure even with a third iteration, or until the convergence of the estimations, but in most of the cases, differences between the second estimation and further estimations are very small.

The Lowess algorithm (Cleveland, 1977) was programmed in the Mathematica language as part of the SEE package. We computed the location and velocity estimations for the x component and the y component of the coordinate time series separately, then combined these estimations to get the two-dimensional estimation for spatial location and velocity. This separation means that a data point that was considered an outlier in one dimension was not necessarily considered an outlier in the other dimension. This procedure, however, suits the photobeam method, since in this method the location of the animal is measured independently in each dimension. The speed (i.e. the absolute length of the velocity

vector) was estimated by computing the square root of the sum of the squares of the velocity estimations in the two dimensions. The smoothed locations were used for computing the spatial spread (see Section 3) and for visualizations (as in Fig. 5).

As in all such methods, Lowess involves a choice of the proper amount of smoothing, which in this case depends on the width chosen for the time window and the degree of the polynomial used for fitting the data within the window. We tested several combinations and settled on a time window 11 points (2.75 s) wide and a 3rd degree polynomial, which seem to eliminate most of the noise while not ironing movement peaks and stops. We tested the segmentation in some of the animals using somewhat different parameters, and there was very little effect on the final results.

It should be noted that Lowess is usually used for estimating general trends in scatter plots with a large noise component. It is, therefore, customary to use a very wide window and only a 1st or 2nd degree polynomial. For our needs of estimating the second derivative in a highly undulating but relatively smooth series, however, a small window is necessary. We found that a higher degree polynomial enabled us to increase this window width somewhat (thus increasing sample size and decreasing the effect of noise and outliers) without over-smoothing. For example, a 3rd degree polynomial can curve twice, thus not eliminating a stop that is much shorter than the 2.75 s duration of the time window. In any case, the degree must be kept considerably lower than the number of data points in the window.

2.3.2. Density estimators

The empirical distributions of speed maxima are presented in this paper using density estimators instead of histograms. Density estimators (Silverman, 1980) are smoothed versions of histograms. They use moving bin location to obtain a more precise estimate of the concentration of observations at a given value. In this way, the discontinuities displayed in the histogram, which are an artificial result of the non-overlapping bins, can be avoided, and better estimates are obtained. The curves obtained through a density estimator involve a choice of proper degree of smoothing. As with choosing the proper bin width for a histogram, we choose in each case the minimal degree of smoothing for which small random fluctuations are smoothed, while genuine features are not ironed away (Silverman, 1980).

2.3.3. The Gaussian Mixture Model

We use the Gaussian Mixture Model to analyze the distribution of speed maxima. This model is used for recognizing distinct components within a population. When subjected to electrophoresis, for example, a mixture of distinct proteins ideally yields a perfect separa-

tion of the mixture into its components, i.e. all the molecules of each component lie precisely at a distance determined by their specific mass. In practice, however, the distance a particular molecule travels is affected by, e.g. convection. As a result, the distances traveled by each type of molecule form a Gaussian. When plotting concentration against distance from origin, one gets a single curve showing peaks corresponding to the medians of each Gaussian. Given a protein mixture, the number of peaks in the curve corresponds to the number of components. The actual proportion of each component can be estimated by fitting a Gaussian Mixture Model to the empirical curve. This model consists of a sum of distinct Gaussians weighted by their corresponding proportions. The proportions of the components in the protein mixture are then calculated by determining the values of the proportions that give maximum likelihood to the model. Note that the method is applicable regardless of whether the individual Gaussians partially overlap.

The parameters of the model are estimated by using the Expectation-Maximization (EM) algorithm (Everitt, 1981). The algorithm estimates the maximum likelihood parameters (proportions, means, and S.D.) of a mixture with a given number of components. EM is an iterative algorithm that starts with user-given initial values, and incrementally improves the likelihood function until further iterations yield only a negligible improvement. The actual number of components of the model is determined by comparing the maximum likelihood value of a n -components mixture with that of a $(n - 1)$ -component mixture until the increased number of components increases the likelihood only marginally (Everitt, 1981). The EM algorithm was programmed in the Mathematica language within the SEE package. We always started with one component and increased the number of components until the increase in the exponent of the likelihood was smaller than 4, which corresponds to a significance level of $P < 0.01$ (see Draï et al., 2000 for details).

3. Results

As expected from the known psychostimulant nature of both drugs, there was a dose-related increase in the activity measured by the photobeam system. The activity (distance traveled) is shown for the PCP injected rats in Fig. 8 and for the AMPH injected group in Fig. 9 (connected dark squares). The activity computed by SEE from the raw data was identical. In the next paragraphs we follow with SEE analysis of the gears in these data.

Fig. 1 demonstrates a typical 2-min time series of movement speed in a 5.0 mg/kg AMPH-injected rat, as estimated by the Lowess algorithm (see Section 2).

Typical time series of the speed in the PCP and saline groups do not seem apparently different. The noise level of speed measurement error was estimated to be 4 cm/s. This is slightly higher than the value of speed that will be measured in the case that one end of the animal's body interrupts a beam for only one time unit (0.25 s in this study). Such speed values might thus be generated by tremor or breathing movements. Each sequence of speeds higher than this threshold was considered as a 'non-arrest' segment, and was represented by the maximum speed that was attained within this segment.

Fig. 2 (left) shows typical distributions of the speed maxima from 60 min sessions of one saline-injected rat, one AMPH rat and one PCP rat, as estimated by density estimation curves (see Section 2). The curves are clearly multi-modal. Fig. 2 (right) shows the best curves given by the Gaussian Mixture Model for these two sessions, together with the best estimation generated for the different components. In both of the cases demonstrated in Fig. 2, three Gaussian components were found to best account for the overall distribution of speed maxima. Note also that the means, variances and proportions of each of the three components of the three rats are similar. We term these components from the left to the right G1, G2 and (when it is present) G3.

Out of 78 animals in this study, 69 (88%) had three significant components. The other nine had only two significant components. Out of 42 animals of the AMPH group, only three had two components, all of them belonging to the saline-injected sub-group. Out of the 46 animals in the PCP group, seven had two components, and they were found in all doses. In both the AMPH and the PCP groups, most of the rats with only two components had low activity, and some did not complete even a one full trip around the 43×43 cm activity cage. In the next section we discuss this variation in the number of components.

The model gives the means and standard deviations of each of the Gaussian components. Usually there is some overlap between nearby components (as in Fig. 2). This means that, with any choice of a threshold between adjacent components, some segments will be misclassified. In order to minimize the number of misclassified segments we define the threshold between subsequent components as the value in which their density curves intersect (Draï et al., 2000).

Fig. 3 displays the estimation generated by the Gaussian Mixture Model for the values of G1 mean, G1/G2 threshold, G2 mean, G2/G3 threshold, and G3 mean (the last two only if there were three components), in four doses of the AMPH-injected rats. The rats within each dose are ordered by an increasing activity, as measured by the overall length of the path. In most animals, G1 mean was at 5 cm/s, G2 mean at 7–10 cm/s, and G3 mean at 15–20 cm/s. There seems to be little effect of dose or activity on these values, except for

a slight tendency to increase G3 mean speed at higher activities or doses. Comparison of group means using an *F*-test (one-way ANOVA) did not find significant differences between doses (all *P* values larger than 0.08) with either gear means or gear thresholds.

Fig. 4 displays the estimations for the same values in the five doses of the PCP-injected rats. Typical values are similar to those found with AMPH, perhaps slightly lower for G2 and G3 means. In this group also, no significant differences were found between doses (all *P* values larger than 0.34) with either gear means or gear thresholds. Also, in each of the PCP doses there were one or two animals with only two components.

As in Drai et al. (2000), after categorizing each non-arrest segment as a G1, G2 or G3 segment, subsequent G1 and arrest segments (which were filtered out at the previous step) were joined together and termed 'lingering' episodes. This is because the distinction between the 'arrest' and G1 categories (i.e. between movements that are considered to be measurement errors and movements which are considered minimal motions of the

animal) is in general very difficult, depending critically on the properties and resolution of the measurement system.

The main finding of Drai et al. (2000) for rats and mice in the large arena was that lingering is actually 'within place' behavior, while G3 segments (and perhaps also G2) are used for progression between different places. That is, although a-priori it is quite possible for the animal to cover a long distance in the lingering mode, in reality it hardly ever does so. Lingering episodes are not only spatially restricted, they also tend to aggregate into specific places, while the distance-covering G3 segments tend to connect these places. This property has also been found in the present study in the photobeam chamber. This is illustrated for one of the 5.0 mg/kg AMPH rats in Fig. 5. The paths and spatial distribution of G2 segments seems to be different from those of both lingering and G3, although their function is not clear yet.

In order to quantify the difference between the distance-covering properties of the three gears we compute the spatial spread of each segment as the maximal

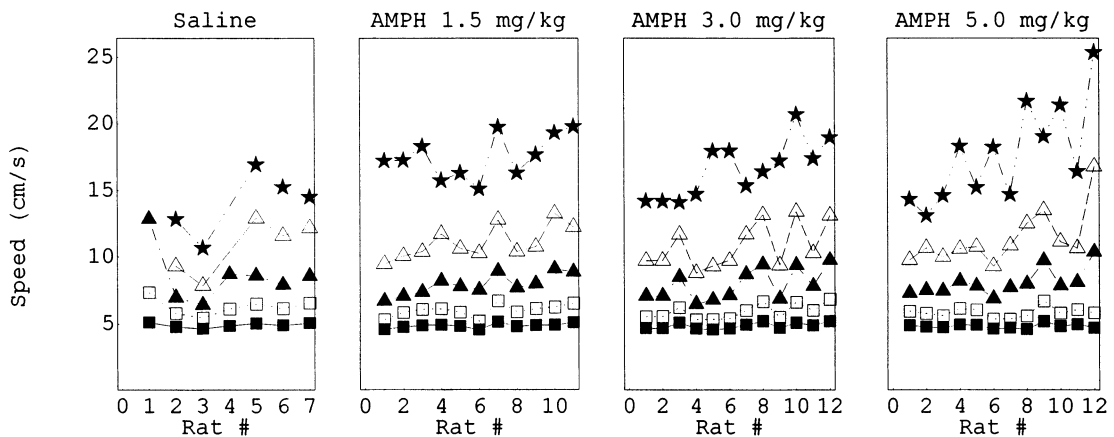


Fig. 3. Values of G1 mean (closed squares), G1/G2 threshold (open squares), G2 mean (close triangles), G2/G3 threshold (open triangles) and G3 mean (closed asterisks) in all the AMPH group rats. The four graphs correspond to doses (from the left) saline, 1.5, 3.0 and 5.0 mg/kg. Animals on the horizontal axis of each graph are ordered according to increasing activity level. Speed units on the vertical axis are cm/s. Animals that had only two significant components do not have values for G2/G3 threshold and G3 mean.

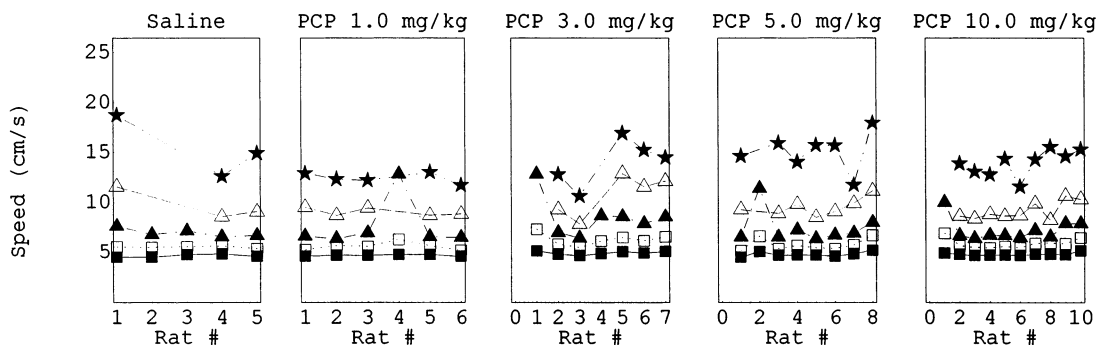


Fig. 4. Values of G1 mean (closed squares), G1/G2 threshold (open squares), G2 mean (close triangles), G2/G3 threshold (open triangles) and G3 mean (closed asterisks) in all the PCP group rats. The five graphs correspond to doses (from the left) saline, 1.0, 3.0, 5.0 and 10.0 mg/kg. Animals on the horizontal axis of each graph are ordered by an increasing activity level. Speed units on the vertical axis are cm/s. Animals that had only two significant components do not have values for G2/G3 threshold and G3 mean.

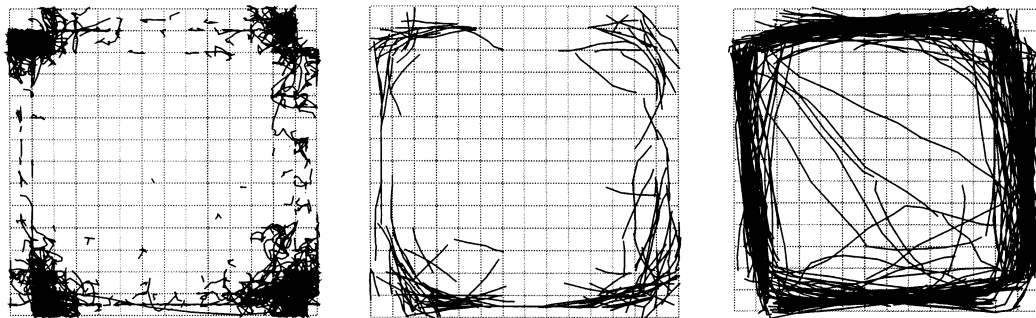


Fig. 5. Smoothed path plots of lingering episodes (left), G2 segments (middle) and G3 segments (right) for a representative AMPH rat in the photobeam chamber. The grid represents the beam locations, 2.54 cm apart, and the resolution of the tracking system is half of this distance, i.e. 1.27 cm, since the coordinate of the animal's center is computed as half the distance between the extreme beam interruptions. The path plots shown here are the result of the same Lowess smoothing used for estimating the speed.

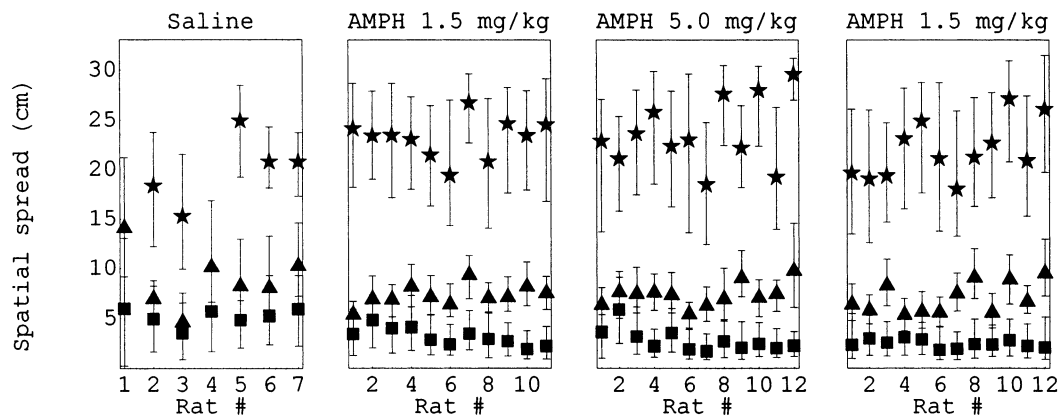


Fig. 6. Values of the median spatial spread of lingering episodes (squares), G2 segments (triangles) and G3 segments (asterisks) in all the AMPH group rats. Bars represent lower and upper quartiles. The four graphs correspond to doses (from the left) saline, 1.5, 3.0 and 5.0 mg/kg. Animals on the horizontal axis of each graph are ordered by an increasing activity level. Distance units on the vertical axis are cm. Animals that had only two significant components do not have values for G3 median.

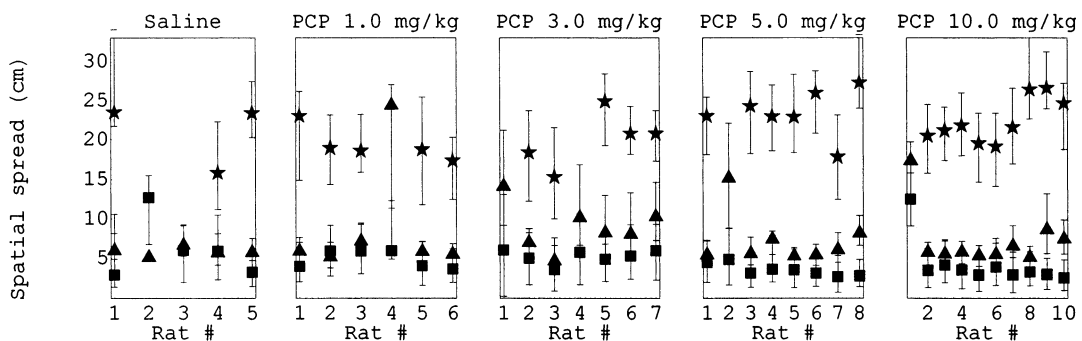


Fig. 7. Values of the median spatial spread of lingering episodes (squares), G2 segments (triangles) and G3 segments (asterisks) in all the PCP group rats. Bars represent lower and upper quartiles. The five graphs correspond to doses (from the left) saline, 1.0, 3.0, 5.0 and 10.0 mg/kg. Animals on the horizontal axis of each graph are ordered by an increasing activity level. Distance units on the vertical axis are cm. Animals that had only two significant components do not have values for G3 median.

distance attained within this segment (i.e. the maximum distance between any two coordinates of the path within this segment). Medians, lower quartiles and upper quartiles of the spatial spread in each component are shown in Fig. 6 (AMPH rats) and Fig. 7 (PCP rats). In most animals, G3 segments typically cover distances of 15–30 cm. That is, more than one body length and

approaching the side length of the arena (43 cm). Lingering episodes, in contrast, typically cover less than 8 cm. G2 segments typically cover 7–12 cm, distinctly different from the G3 segments but somewhat less distinct from the lingering episodes. Note that we know from the outset that there is some overlap between the components, causing certain misclassification. The ‘er-

ror bars' in Figs. 6 and 7 are thus not intended to test the significance of the difference, but only to give a general notion of it.

While the typical speed and segment length within each gear was similar across both drugs and all doses, the number of segments within all gears changed in a dose related fashion with both drugs (Figs. 8 and 9). In other words, most if not all of the considerable hyperactivity induced by both AMPH and PCP did not stem from any increase in the typical segment length in each gear, but rather from the increase in their number. This result is similar to what was earlier found with hyperactivity induced by fimbria-phornix lesion (Whishaw et al., 1994). Using the number of segments within each gear, the discrimination between doses was not better than by using the overall activity (see again Figs. 8 and 9). This discrimination, however, shows that SEE anal-

ysis can dissect general activity into two aspects, one (the number of segments) of which is dose-dependent aspect while the other (segment length) is much more stable across doses, drugs and environments.

4. Discussion

The results shown here support the generality of stops ('lingering episodes') and progression segments (G2 and G3 segments) as the basic units of exploratory locomotor behavior. As shown, the intrinsic distinction between them is independent of arena size, arena shape, the measurement system used and the dose of two psychostimulant drugs. There has been no need for any significant alteration of the segmentation algorithm, developed by Drai et al. (2000) for the analysis of normal behavior measured by a video-tracking system in a 650 cm circular arena, in order to accommodate for drug-induced behavior measured by a photobeam system in a 43 cm square activity cage. The distinction between staying in place and progression is thus very resistant to changes in context, preparation, activity and measurement system.

It is important to clarify that we consider the absence of almost any dose-effect on the values of gear speeds as a support for our claim that these gears constitute basic units of rodent locomotor behavior. This absence of effect allows us to use the gears as the 'primitives' of both normal and drug-induced behavior, and thus enables comparison of the structure of behavior, as constructed of these primitives, across doses. We expect dose effect to be revealed in this structure. For e.g. Figs. 8 and 9 show the dose effect in the number of segments in each gear. We expect also differences, e.g. in the temporal and spatial arrangement of stops and progression segment, which is out of the scope of this paper.

One question raised by these results is why our analysis discovered only two significant components in 12% of the rats. A look at Figs. 4 and 5 reveals that most two-gear animals belong to the saline group (that had a much lower activity than drug-injected groups), or are animals that had a lower activity within their dose group. Some of them did not complete even one full trip around the chamber, and others performed only two or three round trips. There are at least two ways in which low activity could reduce the number of detected gears. The first is that a low-activity animal might never use the third gear at all, or use it so sparingly that its frequency is not significant. In such a case we will expect the second component's mean to be similar to the G2 mean of the three-gear animals, as seems to be the case with, e.g. rats 2 and 3 of the saline sub-group in the PCP group (Fig. 4, leftmost graph).

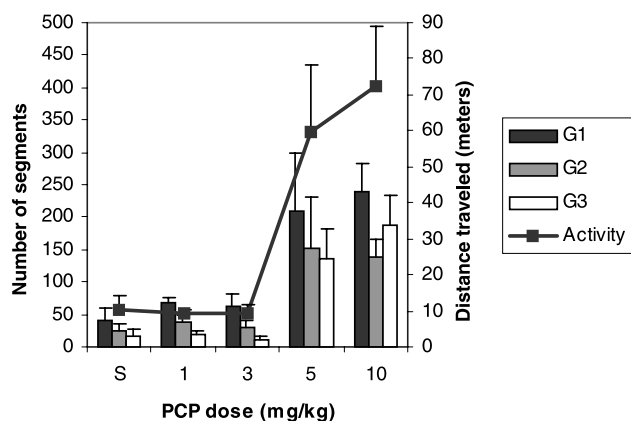


Fig. 8. Distance traveled (group mean \pm S.E., line connected rectangles) in all doses of PCP, and the number of segments performed (group mean \pm S.E.) in each dose in G1 (black bars), G2 (gray bars) and G4 (white bars).

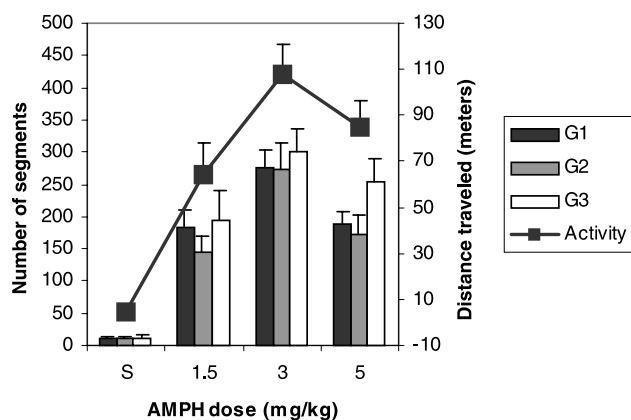


Fig. 9. Distance traveled (group mean \pm S.E., line connected rectangles) in all doses of AMPH, and the number of segments performed (group mean \pm S.E.) in each dose in G1 (black bars), G2 (gray bars) and G4 (white bars).

The second way is that, even if the animal did use all the gears, the sample size (i.e. the overall number of segments) was too small for a significant discrimination of the three components. In some of these animals, the density estimation of the distribution indeed appeared to be clearly tri-modal, yet the Gaussian Mixture Model could discern only two significant components since the overall number of segments was small (less than hundred segments, as opposed to several hundreds or even more than a thousand in active animals). In such a case, there are two likely possibilities—(1) G2 segments are mostly added to the G3 component; in such cases we expect the second component's mean to have an intermediate value between G2 and G3 means of three-gear animals, as may be the case with rat # 1 of the highest PCP dose (Fig. 4, rightmost graph). (2) G2 segments are mostly added to the G1 component. In this case, we expect the mean of the second component, which is in fact G3, to have a value similar to the G3 mean of the three-gear animals. This appears to be the case in rat 4 of the second PCP dose.

Another problem in our results is the poor distinction between the spatial spread of G1 and G2 segments, as opposed to the clear separation between the spatial spread of G2 and G3 segments (see Figs. 6 and 7). This might be explained by the low resolution of the photobeam system with movements that are smaller than one body length. The spatial resolution of the photobeam system in this study is somewhat lower than the spatial resolution of the video tracking in a large arena, one beam per 2.54 cm distance, compared with about one pixel per 1.50 cm. In addition, the animal's coordinate in the photobeam system is computed as the middle between the extreme points in each of the x and y dimensions. In the video tracking system the animal's coordinate, in contrast, is computed as the 'center of gravity' of all the animal's pixels. A computation based on all of the animal's detected points is likely to have a better resolution for small movements than a computation based on only the extreme points. If, for example, the animal is bending to one side, the photobeam system is likely to record a larger movement than the video tracking system. Moreover, since the computation is done separately for each dimension, the same bending might produce different movement amplitudes as a function of the animal's orientation, while with the center of gravity method the animal's orientation does not influence the measurement.

Note in Figs. 6 and 7 that the separation between the spatial spreads of G1 and G2 seems to increase with higher doses (which generally produced higher activity in this study) and higher levels of activity within the same dose. This suggests that the separation is real, and is better detected when the sample size (and thus discrimination between components) is increased.

Estimated speed values for G1, G2 and G3 measured

for normal rats in the large arena are several times higher than those measured in this study for both saline and drug-injected rats in the small photobeam cage. Whereas typical values for the respective means of the three components are 10, 25 and 100 cm/s in the large arena, they amount to 5, 8 and 16 cm/s in the photobeam cage. It is unlikely rats can develop speeds of 100 cm/s (with maximal values as high as 300 cm/s) in a 45-cm chamber. This raises the question of the relation between the three gears found in the two respective environments. One explanation could be that there are in fact four gears, of which only the slower three are used in the photobeam cage and the faster three in the large arena. Another explanation is that the animals scale the typical speeds of the gears to fit the arena's size, much as they scale the inter-stop distance (Golani et al., 1993). This issue should be reconciled by future studies with arenas of intermediate sizes. A scaling will support our hypothesis that the gears are not merely motor, but rather cognitive in their nature. That is, that they do not reflect, for example, different gaits. It should be noted that our preliminary investigation of rats that were simultaneously filmed by an additional 'close-up' synchronized camera (data from Tchernichovski et al., 1989) could not find a correlation between gears and gates. Rather, we hypothesize that the gears reflect a cognitive structure: the distribution of animal-defined 'places' in the environment and their connectivity.

The notion of place plays a central roll in the neurosciences, in place learning (e.g. Morris, 1984; Whishaw, 1998; Silva et al., 1998), navigation (Thinus-Blanc, 1996; Etienne et al., 1998; Knierim et al., 1998), and the study of several brain regions, especially the hippocampus (McNaughton et al., 1996; Poucet and Bemhamou, 1997; O'keefe and Burgess, 1996). There is as yet, however, no algorithmic definition of the behavior that marks 'a place'. We suggest that G1 consists of movements that are done within places, while G3 consists of movements that connect different places. The roll of G2 is not clear yet, but at least in this case it seem to consist of movement in the range of one body length that are still confined to one place (see Fig. 5). Thus, G1 can be used to study the properties and development of places, while G3 can be used to study the connectivity of places and the formation of cognitive maps. These questions, however, are best studied in a large arena, where the resolution obtained by video tracking is much higher, where the number of possible places and the range of possible speed are much larger, and where the basic organization of the behavior was already studied. The photobeam cage is a less appropriate setting to study such questions, but it has the advantages of being smaller, easy to use and readily available in many laboratories. SEE analysis of photo-

beam data has thus the potential to improve the resolution of many studies in psychopharmacology.

It is interesting to note that the large-scale organization of both saline and drug-induced behavior in this study appeared to be different from the well-known organization of rat exploratory behavior in a large arena. Especially, the process of gradual growth in the range of excursions from the home-base seemed to be much less distinctive. This is of course understandable, regarding that there is a much less room for exploratory expansion in a 43×43 cm chamber, and that the animal can easily see the whole chamber in one glance. A visualization of this large-scale organization using SEE does reveal, however, interesting and complex patterns that will be described in future papers. Regarding this difference, the similarity in the existence of the three gears supports our notion that they are basic and natural units of rodent spatial behavior, from which different large-scale patterns of behavior may be composed.

Acknowledgements

This research was supported by a grant from Novartis. The SEE package is available from the authors upon request, but requires the Mathematica programming environment.

References

- Cleveland WS. Robust locally weighted regression and smoothing scatterplots. *J Am Stat Assoc* 1977;74:829–36.
- Cools AR, Ellenbroek BA, Gingras MA, Engbersen A, Heeren D. Differences in vulnerability and susceptibility to dexamphetamine in Nijmegen high and low responders to novelty: a dose-effect analysis of spatio-temporal programming of behavior. *Psychopharmacology* 1997;132:181–7.
- Drai D, Golani I. SEE: a tool for the visualization and analysis of rodent exploratory behavior. *Neurosci Biobehav Rev*, in press.
- Drai D, Benjamini Y, Golani I. Statistical discrimination of natural modes of motion in rat exploratory behavior. *J Neurosci Methods* 2000;96(2):119–31.
- Eilam D, Golani I. Home base behavior of rats (*Rattus norvegicus*) exploring a novel environment. *Behav Brain Res* 1989;34:199–211.
- Etienne AS, Maurer R, Berlie J, Reverdin B, Rowe T, Georgakopoulos J, Seguinot V. Navigation through vector addition. *Nature* 1998;396(6707):161–4.
- Everitt BS. *Finite Mixture Distributions*. London: Chapman & Hall, 1981.
- Gingras MA, Cools AR. Different behavioral effects of daily or intermittent dexamphetamine administration in Nijmegen high and low responders. *Psychopharmacology* 1997;132:188–94.
- Golani I, Benjamini Y, Eilam D. Stopping behavior: constraints on exploration in rats (*Rattus norvegicus*). *Behav Brain Res* 1993;53:21–33.
- Knierim JJ, Kudrimoti HS, McNaughton BL. Interactions between idiothetic cues and external place cells and head direction cells. *J Neurophysiol* 1998;80(1):425–46.
- McNaughton BL, Barnes CA, Gerrard JL. Deciphering the hippocampal polyglot: the hippocampus as a path integration system. *J Exp Biol* 1996;199:173–85.
- Morris R. Developments of a water-maze procedure for studying spatial learning in the rat. *J Neurosci Methods* 1984;11(1):47–60.
- O'keefe J, Burgess N. Geometric determination of the place fields of hippocampal neurons. *Nature* 1996;381(6581):425–8.
- Paulus MP, Geyer MA. A temporal and spatial scaling hypothesis for the behavioral effects of psychostimulants. *Psychopharmacology (Berl)* 1991;104(1):6–16.
- Paulus MP, Geyer MA, Gold LH, Mandel AJ. Application of entropy measures derived from the ergodic theory of dynamical systems to rat locomotor behavior. *Proc Natl Acad Sci USA* 1990;87(2):723–7.
- Poucet B, Bemhamou S. The neuropsychology of spatial cognition in the rat. *Crit Rev Neurobiol* 1997;11(2-3):101–20.
- Silva AJ, Giese KP, Fedorov NB, Frankland PW, Kogan JH. Molecular, cellular, and neuroanatomical substrates of place learning. *Neurobiol Learning Memory* 1998;70(1-2):44.
- Silverman BW. *Density Estimation for Statistics and Data Analysis*. London: Chapman & Hall, 1980.
- Szechtman H, Sulis W, Eilam D. Quinpirole induces compulsive checking behavior in rats: A potential animal model of obsessive-compulsive disorder (OCD). *Behav Neurosci* 1998;112(6):1475–85.
- Tchernichovski O, Golani I. A phase plane representation of rat exploratory behavior. *J Neurosci Methods* 1995;62(1-2):21–7.
- Tchernichovski O, Benjamini Y, Golani I. The dynamics of long term exploratory behavior in the rat, part I. *Biol Cybern* 1989;78(6):423–32.
- Thinus-Blanc C. *Animal Spatial Cognition: Behavioral and Brain Approach*. Singapore: World Scientific, 1996.
- Whishaw IQ. Place learning in hippocampal rats and the path integration hypothesis. *Neurosci Biobehav R* 1998;22(2):209–20.
- Whishaw IQ, Coles BLK, Bellerive CHM. Food carrying-A new method for naturalistic studies of spontaneous and forced alternation. *J Neurosci Methods* 1995;61:139–43.
- Whishaw IQ, Cassel JC, Majchrzak M, Cassel S, Will B. “Short-stops” in rats with fimbria-fornix lesions: evidence for change in the mobility gradient. *Hippocampus* 1994;4(5):577–82.